Eur. Phys. J. D **41**, 403–411 (2007)
DOI: 10.1140/epjd/e2006-00228-6

THE EUROPEAN PHYSICAL JOURNAL D

The influence on atomic decay by inserting a LHM layer into an ordinary one dimensional multi-layer structure

J.P. Xu[1,2,a], Y.P. Yang[1], N.H. Liu[2,3], and S.Y. Zhu[2,4]

[1] Department of Physics, Tongji University, Shanghai 200092, P.R. China
[2] Department of Physics, Hong Kong Baptist University, Kowloon Tong, Hong Kong
[3] Department of Physics, Nanchang University, Nanchang 330047, P.R. China
[4] Key Laboratory of Quantum Communication and Quantum Computation, University of Science and Technology of China, Hefei 230026, P.R. China

Received 27 February 2006 / Received in final form 5 June 2006
Published online 13 October 2006 –

Abstract. Inserting left-handed material (LHM) layers into a one dimensional structure can influence the spontaneous emission (SpE) of a two-level atom. This has been investigated, starting from the simplest case of a three-layer system, where we find the reflected field (atom can "see") passing through LHM layer is stronger than that through the corresponding normal layer. Indeed the induced decay is more strongly influenced by reflected field passing through LHM layer. Based on this and after further analysis of reflectivity, we find that, a quarter photonic crystal (PC) composed of alternately LHM and RHM can inhibit the atomic spontaneous emission more intensely compared to an ordinary PC.

PACS. 42.25.Bs Wave propagation, transmission and absorption – 42.50.Lc Quantum fluctuations, quantum noise, and quantum jumps – 42.70.Qs Photonic bandgap materials

1 Introduction

Recently a new type of material called left-handed materials (LHM) [1] has attracted considerable attention. In 1968, Veselago [1] first suggested the concept of LHM, which refers to a material processing a negative refractive index with the permittivity and the permeability being negative simultaneously. The wave vector is anti-parallel to the direction of energy flow, and the electric field, magnetic field and the wave vector form a left-handed triplet. Some unusual phenomena, such as reverse Doppler shift, reverse Cerenkov radiation, negative refraction, reverse light pressure et al. are expected in LHM. Experimentally, LHM had been realized in the microwave band [2–4]. As the result, its most potential application of the LHM, the perfect lens which can focus both propagation waves and the evanescent waves, has been predicted [5]. In addition, Li et al. pointed out that a stack composed of alternating LHM layers and normal dielectric (RHM) layers can give rise to a new type of band gap with novel properties [6].

In 1946, Purcell [7] pointed out that the atomic spontaneous decay rate can be enhanced by putting the atom in a cavity. Since then, how to inhibit or enhance atomic SpE has became an interesting subject. Most research has focused on the inhibition of the atomic SpE, because it prolongs the atomic coherent time and is useful in quantum computation and quantum information applications. The effective way to realize this is to put the atom into a micro-cavity or a PC [8–10], because the density of states in these environments can be controlled easily by varying the dimension and other parameters of the structure. If we introduce LHM layers into a multi-layer structure, what are the influences of the LHM layers on atomic decay comparing with the influence of the RHM layer. Here we define the PC containing alternate the LHM and the RHM layers as LHM-RHM PC, and the PC containing only the RHM layers as ordinary PC. After analyzing the reflected field emitted by the atom from different interfaces in detail, we find that LHM layers have a stronger influence on the atomic decay.

This paper is organized as follows: in Section 2, we introduce the model and the interaction Hamiltonian. The different influences of LHM from RHM in a three-layer structure on the atomic decay have been analyzed in Section 3. The case in a PC is presented in Section 4. Finally we give the conclusion in Section 5.

2 Model and interaction Hamiltonian

The 1D LHM-RHM PC without dispersion and dissipation is shown in Figure 1. A two-level atom (transition

[a] e-mail: xx_jj_pp1980@yahoo.com.cn

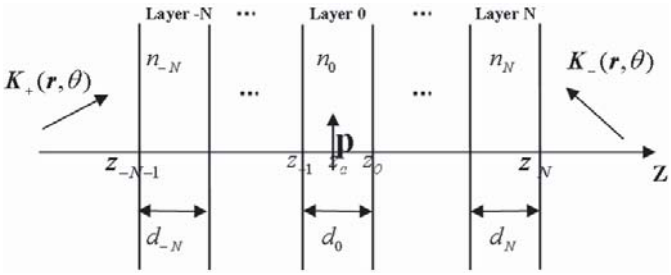

Fig. 1. Sketch of the LHM-RHM 1DPC structure.

frequency ω_0, position $\mathbf{r}_a(0,0,z_a)$ and dipole moment $\mathbf{p}$) is placed in the middle layer (layer 0). In order to have a comparison between the LHM and the RHM, absolute values of the permittivity and the permeability for the RHM layers and for the LHM layers are set be equal. The center of the structure is the origin of the z-coordinate. Each layer is isotropic and in the x-y plane. Though most LHM are anisotropic in experiments [2,3], however isotropic LHM have been realized recently [4]. Other parameters of the structure are shown in Figure 1. Note that the middle layer is set to be vacuum in order to be consistent with the real-cavity model [11–13].

Now we introduce the quantization of the three dimensional electromagnetic field in the presence of the 1DPC. The positive frequency part of the electric field operator for our system can be written as

$$E^{(+)}(\mathbf{r},t) = \sum_{\mathbf{K}_+,\lambda} U(K_+,\lambda,\mathbf{r})\hat{\mathbf{e}}_+\xi_K^m a_{\mathbf{K}_+\lambda}e^{-i\nu_K t} + \sum_{\mathbf{K}_-,\lambda} U(K_-,\lambda,\mathbf{r})\hat{\mathbf{e}}_-\xi_K^m a_{\mathbf{K}_-\lambda}e^{-i\nu_K t} \quad (1)$$

where ν_K is the frequency of $K_\pm$ and $\xi_K^m = (\hbar\nu_K/2|\varepsilon_m|V)^{1/2}$ with m determined by the position $\mathbf{r}$ and ε_m be the permittivity of the mth layer. $U(\mathbf{K}_+,\mathbf{r})$, $U(\mathbf{K}_-,\mathbf{r})$ are the modified mode function in the presence of the 1D structure. According to the quantization scheme in reference [14], the mode functions together with the field unit vectors $(\hat{\mathbf{e}}_+,\hat{\mathbf{e}}_-)$ is expressed as the following piecewise functions, which

$$U(\mathbf{K}_+,\lambda,\mathbf{r})\hat{\mathbf{e}}_+ = \begin{cases} [e^{i\mathbf{K}_{m+}\cdot\mathbf{r}}\hat{\mathbf{e}}_m(\mathbf{K}_+,\lambda) \\ +R_R^\lambda e^{i\mathbf{K}_{m-}\cdot\mathbf{r}+2iK_z z_{-N-1}}\hat{\mathbf{e}}_m(\mathbf{K}_-,\lambda)], & z < z_{-N-1} \\ t_{Lm}^\lambda e^{iK_z z_{-N-1}}[e^{i\mathbf{K}_{m+}\cdot\mathbf{r}-iK_{mz}z_{m-1}}\hat{\mathbf{e}}_m(\mathbf{K}_+,\lambda) \\ +r_{Rm}^\lambda e^{i\mathbf{K}_{m-}\cdot\mathbf{r}+iK_{mz}(z_{m-1}+2d_m)}\hat{\mathbf{e}}_m(\mathbf{K}_-,\lambda)]/D_m^\lambda, & z_{m-1} \le z < z_m \\ T_L^\lambda e^{i\mathbf{K}_{m+}\cdot\mathbf{r}+iK_z(z_{-N-1}-z_N)}\hat{\mathbf{e}}_m(\mathbf{K}_+,\lambda), & z \ge z_N \end{cases} \quad (2)$$

and

$$U(\mathbf{K}_-,\lambda,\mathbf{r})\hat{\mathbf{e}}_- = \begin{cases} [e^{i\mathbf{K}_{m-}\cdot\mathbf{r}}\hat{\mathbf{e}}_m(\mathbf{K}_-,\lambda) + R_L^\lambda e^{i\mathbf{K}_{m+}\cdot\mathbf{r}-2iK_z z_N}\hat{\mathbf{e}}_m(\mathbf{K}_+,\lambda)], & z \ge z_N \\ t_{Rm}^\lambda e^{-iK_z z_N}[e^{i\mathbf{K}_{m-}\cdot\mathbf{r}+iK_{mz}z_m}\hat{\mathbf{e}}_m(\mathbf{K}_-,\lambda) \\ +r_{Lm}^\lambda e^{i\mathbf{K}_{m+}\cdot\mathbf{r}+iK_{mz}(2d_m-z_m)}\hat{\mathbf{e}}_m(\mathbf{K}_+,\lambda)]/D_m^\lambda, & z_{m-1} \le z < z_m \\ T_R^\lambda e^{i\mathbf{K}_{m-}\cdot\mathbf{r}+iK_z(z_{-N-1}-z_N)}\hat{\mathbf{e}}_m(\mathbf{K}_-,\lambda), & z < z_{-N-1} \end{cases} \quad (3)$$

where

$$\mathbf{K}_{m\pm} = (K_x, K_y, \pm K_{mz}) = K(\sin\theta\cos\phi, \sin\theta\sin\phi, \pm n_m\cos\theta_m). \quad (4)$$

Here the angle θ_m is determined by the angle θ in vacuum according to Snell's law

$$\sin\theta = n_m\sin\theta_m. \quad (5)$$

The superscript λ = TE, TM indicates two transverse polarization directions, whose unit vectors are defined as

$$\begin{cases} \hat{\mathbf{e}}_m(\mathbf{K}_\pm,\mathrm{TE}) = (\sin\phi, -\cos\phi, 0), \\ \hat{\mathbf{e}}_m(\mathbf{K}_\pm,\mathrm{TM}) = (\cos\theta_m\cos\phi, \cos\theta_m\sin\phi, \mp\sin\theta_m). \end{cases} \quad (6)$$

In the expressions of the mode functions (2) and (3), $t_{L/Rm}^\lambda$ denotes the transmission coefficient through the left/right part of the mth layer ($z_{m-1} < z < z_m$), $r_{R/Lm}^\lambda$ denotes the reflective coefficient on the right/left interface of the mth layer. $T_{R/L}^\lambda$ denotes the total transmission coefficient of the entire structure coming from the right/left interface of the region of $z < z_{-N-1}/z > z_N$. $R_{R/L}^\lambda$ denotes the total reflective coefficient on the right/left interface of the region of $z < z_{-N-1}/z > z_N$. D_m^λ originates from the multi-reflection effect in the mth layer,

$$D_m^\lambda = 1 - r_{Lm}^\lambda r_{Rm}^\lambda e^{2iK_{mz}d_m}. \quad (7)$$

So the interaction Hamiltonian in the interaction picture is

$$V_I(t) = \hbar\sum_{\mathbf{K}_+,\lambda}[g_{\mathbf{K}_+}^\lambda(\mathbf{r}_a)\sigma_+ a_{\mathbf{K}_+\lambda}e^{i(\omega_0-\nu_K)t} + H.C.] + \hbar\sum_{\mathbf{K}_-,\lambda}[g_{\mathbf{K}_-}^\lambda(\mathbf{r}_a)\sigma_+ a_{\mathbf{K}_-\lambda}e^{i(\omega_0-\nu_K)t} + H.C.] \quad (8)$$

where $g_{\mathbf{K}_\pm}^\lambda(\mathbf{r}_a)$ are the atom-field coupling coefficients,

$$g_{\mathbf{K}_+}^\lambda(\mathbf{r}_a) = -\frac{\xi_K^0}{\hbar}(t_{L0}^\lambda/D_0^\lambda)e^{i\mathbf{K}_+\cdot\mathbf{r}_a+iK(z_{-N-1}+d_0/2)\cos\theta} \times[\mathbf{p}\cdot\hat{\mathbf{e}}_0(\mathbf{K}_+,\lambda) + \mathbf{p}\cdot\hat{\mathbf{e}}_0(\mathbf{K}_-,\lambda)r_{R0}^\lambda e^{-iK(2z_a-d_0)\cos\theta}], \quad (9)$$

$$g_{\mathbf{K}_-}^\lambda(\mathbf{r}_a) = -\frac{\xi_K^0}{\hbar}(t_{R0}^\lambda/D_0^\lambda)e^{i\mathbf{K}_-\cdot\mathbf{r}_a+iK(d_0/2-z_N)\cos\theta} \times[\mathbf{p}\cdot\hat{\mathbf{e}}_0(\mathbf{K}_-,\lambda) + \mathbf{p}\cdot\hat{\mathbf{e}}_0(\mathbf{K}_+,\lambda)r_{L0}^\lambda e^{iK(2z_a+d_0)\cos\theta}]. \quad (10)$$

$$\frac{\Gamma_{||}}{\Gamma_0} = \frac{3}{8} n_0 \mu_0 \int_0^{\pi/2} d\theta \sin\theta \left\{ \left| \frac{t_{L0}^{TE}}{D_0^{TE}} \right|^2 \left| 1 + r_{R0}^{TE} e^{in_0 k_0 (d_0 - 2z_a)\cos\theta} \right|^2 + \left| \frac{t_{L0}^{TM}}{D_0^{TM}} \right|^2 \cos^2\theta \left| 1 + r_{R0}^{TM} e^{in_0 k_0 (d_0 - 2z_a)\cos\theta} \right|^2 + \left| \frac{t_{R0}^{TE}}{D_0^{TE}} \right|^2 \left| 1 + r_{L0}^{TE} e^{in_0 k_0 (d_0 + 2z_a)\cos\theta} \right|^2 + \cos^2\theta \left| \frac{t_{R0}^{TM}}{D_0^{TM}} \right|^2 \left| 1 + r_{L0}^{TM} e^{in_0 k_0 (d_0 + 2z_a)\cos\theta} \right|^2 \right\}, \quad (17a)$$

$$\frac{\Gamma_{\perp}}{\Gamma_0} = \frac{3}{4} n_0 \mu_0 \int_0^{\pi/2} d\theta \sin^3\theta \left\{ \left| \frac{t_{L0}^{TM}}{D_0^{TM}} \right|^2 \left| 1 - r_{R0}^{TM} e^{in_0 k_0 (d_0 - 2z_a)\cos\theta} \right|^2 + \left| \frac{t_{R0}^{TM}}{D_0^{TM}} \right|^2 \left| 1 - r_{L0}^{TM} e^{in_0 k_0 (d_0 + 2z_a)\cos\theta} \right|^2 \right\} \quad (17b)$$

The state vector of the system is

$$|\psi_I(t)\rangle = C_a(t)\,|a,0\rangle + \sum_{\mathbf{K}_+,\lambda} C_{b\mathbf{K}_+\lambda}(t)\,\left|b, 1_{\mathbf{K}_+\lambda}\right\rangle + \sum_{\mathbf{K}_-,\lambda} C_{b\mathbf{K}_-\lambda}(t)\,\left|b, 1_{\mathbf{K}_-\lambda}\right\rangle. \quad (11)$$

The state $|a,0\rangle$ refers to the atom in the excited state with no photon, and $\left|b, 1_{\mathbf{K}_\pm\lambda}\right\rangle$ refers to the atom in the ground state with one photon in the mode of $(\mathbf{K}_\pm, \lambda)$. We assume initially, $C_a(0) = 1$ and $C_{b\mathbf{K}_\pm\lambda}(0) = 0$. Solving the Schrödinger equation in the interaction picture

$$\frac{\partial}{\partial t}|\psi_I(t)\rangle = -\frac{i}{\hbar} V_I\,|\psi_I(t)\rangle \quad (12)$$

with a standard deduction, the equation of atomic upper level probability amplitude can be obtained [15]

$$\dot{C}_a(t) = -\left[\sum_{\mathbf{K}_+,\lambda} |g_{\mathbf{K}_+}^{\lambda}(\mathbf{r}_a)|^2 + \sum_{\mathbf{K}_-,\lambda} |g_{\mathbf{K}_-}^{\lambda}(\mathbf{r}_a)|^2 \right] \times \int_0^t dt' e^{i(\omega_0 - \nu_K)(t-t')} C_a(t'). \quad (13)$$

Now transforming the summation over K_+ and K_- into an integral, which gives

$$\sum_{\mathbf{K}_\pm} \to \frac{V}{(2\pi)^3} \int d\mathbf{K}_\pm = \frac{V}{(2\pi)^3} \int_0^\infty dK \int_0^{\pi/2} d\theta \int_0^{2\pi} d\phi K^2 \sin\theta. \quad (14)$$

Equation (13) becomes

$$\dot{C}_a(t) = -\frac{V}{(2\pi)^3} \int_0^t dt' C_a(t') \int_0^\infty dK K^2 e^{ic(k_0 - K)(t-t')} \times \int_0^{2\pi} d\phi \int_0^{\pi/2} d\theta \sin\theta \sum_{\lambda=TE}^{TM} [|g_{\mathbf{K}_+}^{\lambda}(\mathbf{r}_a)|^2 + |g_{\mathbf{K}_-}^{\lambda}(\mathbf{r}_a)|^2], \quad (15)$$

where $k_0 = \omega_0/c$ and $K = \nu_K/c$.

With the Weissikopf-Wigner approximation [15] ($t \gg 1/\omega_0$), equation (15) can be reduced to

$$\dot{C}_a(t) = -\frac{\Gamma}{2} C_a(t) \quad (16)$$

where Γ is the steady decay rate and depends on the atomic polarization and position. If the atomic dipole is along the x-axis, $\mathbf{p} = p(1,0,0)$, we have $\Gamma = \Gamma_{||}$

see equation (17a) above

where Γ_0 is the decay rate in the free space (the vacuum). If the atomic dipole is perpendicular to the interfaces of the layers, i.e. $\mathbf{p} = p(0,0,1)$, we have $\Gamma = \Gamma_\perp$

see equation (17b) above.

It is well-known that atomic spontaneous emission is related to its environment. In current case, the environment is represented by the reflection and transmission coefficients.

3 Three-layer case

In order to see the difference on the atomic decay in the ordinary PC and in the LHM-RHM PC, we consider the symmetric three-layer structure (0|A|0|A|0) first. Here "|" indicates the interface between two materials. The "0" refers to the vacuum layers, and the "A" refers to the layers with thickness d_A and refractive index n_A. The atom is at the center of the middle layer $z_a = 0$ and the thickness of it is d_0.

In the following we consider the special LHM and RHM for layer A, the absolute refractive index equals to 1 ($\varepsilon_A = 1/\mu_A$ and $\varepsilon_A \neq 1$). For the atomic dipole along the x-axis, $\mathbf{p} = p(1,0,0)$, the steady decay rate can be decomposed as follows under the condition of $t \gg 1/\omega_0$

$$\Gamma \approx \Gamma_0 \tag{a}$$

$$+\frac{3}{2}\Gamma_0 \mathrm{Re}\sum_{m=1}^{2}(-r_0)^m e^{imk_0d_0}\left[\frac{2}{imk_0d_0}+\frac{2}{(mk_0d_0)^2}-\frac{2}{i\,(mk_0d_0)^3}\right] \tag{b}$$

$$+\frac{3}{2}\Gamma_0 \mathrm{Re}\sum_{m=1}^{2}(t_0^2r_0)^m e^{im(2n_Ak_0d_A+k_0d_0)}\left[\frac{2}{im(2n_Ak_0d_A+kd_0)}+\frac{2}{m^2(2n_Ak_0d_A+kd_0)^2}-\frac{2}{im^3(2n_Ak_0d_A+k_0d_0)^3}\right] \tag{c}$$

$$+\frac{3}{2}\Gamma_0 \mathrm{Re}\sum_{m=1}^{2}(-2t_0^2r_0^2)^m e^{im(2n_Ak_0d_A+2k_0d_0)}\left[\frac{2}{i(2n_Ak_0d_A+2k_0d_0)}+\frac{2}{(2n_Ak_0d_A+2k_0d_0)^2}-\frac{2}{i(2n_Ak_0d_A+2k_0d_0)^3}\right] \tag{d}$$

$$+\ldots \tag{18}$$

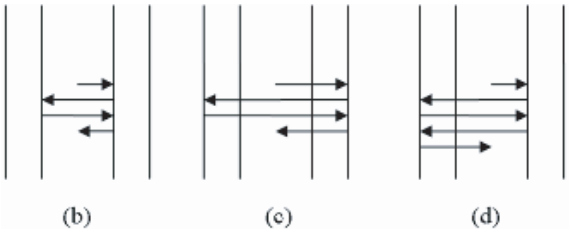

Fig. 2. The path of each term in equation (18).

(see the Appendix)

see equation (18) above

where r_0 is the Fresnel reflectivity incident from layer A to vacuum for the TE wave, t_0^2 is expressed in equation (A.8) (detailed deductions are shown in the Appendix). Here the Lamb shift is neglected. Each term in equation (18) represents the contribution of the reflected fields back to the atom with the different paths. The terms (b), (c) and (d) are shown in Figure 2. Term (a) describes the free decay which is immune to the surroundings; term (b) describes the contribution of the field reflected at the nearest interfaces; term (c) represents the contribution reflected at the outside interfaces; term (d) the contribution reflected from one nearest interface and its opposing outer interface.

From equation (18), the induced decay rate (terms (b), (c) and (d)) caused by the reflected field is mainly inversely proportional to the phase shift. Furthermore, x^{-1}, x^{-2} and x^{-3} in each term correspond to the dipole radiation field, the induced field and the electrostatic field respectively. In the LHM, the phase shift decreases with wave propagation. On the other hand, the phase shift is always increasing in RHM. Finally the reflected field passing through LHM layer is stronger in amplitude than that through RHM layers, which leads to a more intense change in the decay rate. As the reflectivity and transmitted coefficients (r_0, t_0^2) at the interface are the same for both the LHM and RHM cases, from equation (18), the only difference between LHM and RHM is the phase shift ($mn_Ak_0d_A + lk_0d_0$, m and l are arbitrary integrals). The effect of the RHM or the LHM layer A on SpE can be summarized as follows.

Firstly, terms (b), (c) and (d) will be small enough that they can be omitted as d_0 tends to infinity, and consequently only term (a) will contribute to the decay, which is just as in free space, $\Gamma \approx \Gamma_0$. Secondly, term (b) is identical for the LHM and the RHM, because it don't include the contribution of the reflected field passing through layer A. Thirdly, term (c) is smaller than (b) for RHM case, because the denominator of (c) is larger than (b). However, for LHM layer, i.e. $n_A < 0$, the denominator $|m(2n_Ak_0d_A + n_0k_0d_0)|$ can be smaller than $|mk_0d_0|$, in which case the contribution of term (c) will be larger than that of term (b). Consequently, the reflected field through the LHM layer is stronger than that through the RHM layer, which leads to stronger effect on the decay rate. Finally, terms (c) and (d) can be neglected when d_A is large enough, and so the difference between LHM and RHM will disappear. That means layer 0 is connected to two half-infinite layers.

There also exist many other contributions of the reflected field along other paths. They must be much weaker than terms (b), (c) and (d) for the RHM case (due to $|r_0| < 1$ and a larger phase shift). However, for the LHM case, they may be equal to or even larger than terms (b), (c) and (d) due to the phase compensation effect of the LHM layer. We neglect them here in order to be concision.

Now we perform the numerical calculations according to equation (17a) to confirm the deductions made above. Layers A with thickness d_A can be LHM ($\varepsilon_A = -0.25$ and $\mu_A = -4$) or RHM ($\varepsilon_A = +0.25$ and $\mu_A = +4$). From equation (18), we know that the thickness of layer A plays the dominant role in distinguishing between the effect of LHM and RHM. So we plot the SpE rate as function of d_A according to equation (17a) in Figure 3 with fixed d_0.

From Figure 3, the normalized decay rate oscillates with d_A. The oscillation is caused by the periodically variation of the reflectivity with increasing d_A. In other words, the density of states changes periodically with d_A.

Because the intensity of the reflected field passing through LHM layer back to atom is stronger than that passing through RHM, the superposition of the reflected field and the emitted field in LHM case can have stronger constructive or deconstructive interference. In Figure 3,

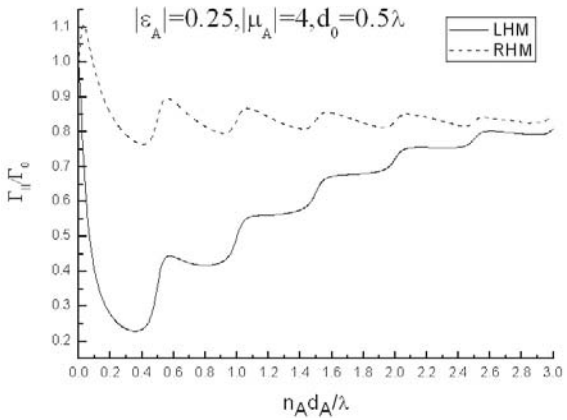

Fig. 3. The normalized decay rate as function of d_A. Solid line for the LHM layer A, dashed line for the RHM layer A.

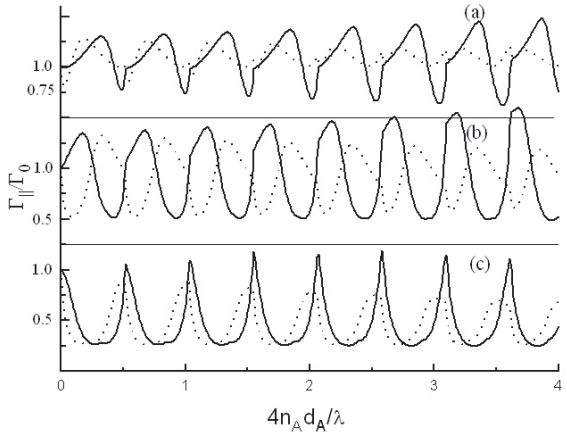

Fig. 4. The decay rate as function of d_A, (a) for $d_0 = 0.75\lambda_0$, (b) for $d_0 = 0.5\lambda_0$, (c) for $d_0 = 0.25\lambda_0$. Solid line for the LHM layer A, dashed line for the RHM layer A.

the stronger deconstruction (deeper inhibition) is presented. The difference between the RHM and the LHM layers will disappear as $d_A \gg 3\lambda_0$.

A similar result will be obtained if the index of layer A $|n_A| \neq 1$. For example, we plot the decay rate versus d_A in Figure 4 for layer A of LHM ($\varepsilon_A = -8$ and $\mu_A = -2$) or of RHM ($\varepsilon_A = +8$ and $\mu_A = +2$). The change of the decay rate (the difference between the decay rate and the free space decay rate) for LHM (solid line) is larger than that for RHM (dashed line), see Figure 4. The amplitude of the change of SpE rate for LHM increases linearly with d_A, while decreases for RHM.

There is always a focal point of the reflected field to the left of the LHM with $n_A = -1$ according to Snell's law, see Figure 5a. The position of the focus will leave away from the interface with increasing d_A. The intensity of the reflected field is strongest at the focus. So the change of decay rate is largest when $d_A \approx d_0$, as shown by the solid line in Figure 3.

However, when $n_A \neq -1$, there is no clear focal point of reflected field, as shown in Figure 5b. Due to the non-perfect focus of reflected field in the case of Figure 4, the

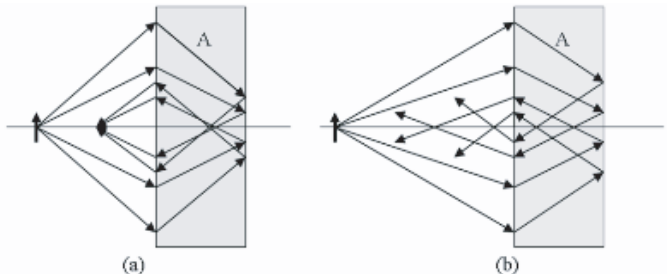

Fig. 5. (a) A perfect focusing of the reflected field as $n_A = -1$, (b) non-perfect focusing of the reflected field as LHM's index $n_A \neq -1$ (we omit other reflected paths including transmission to the right and multi-reflection).

tendency to increase for LHM is longer than in Figure 3. The decay rate in Figure 4 will have the same value for the LHM and the RHM at a much larger d_A compared with the case of Figure 3.

4 Photonic crystals

The method giving equation (18) only fits for the simplest case. For more a complicated case, such as in a PC with an arbitrary refractive index, the decay rate cannot be decomposed into the formation in equation (18), because the integral over an angle is impossible to resolve analytically. However, equation (18) provides us with a clear physical picture to distinguish the different influences of the LHM layer from the RHM layer on the atomic decay. We can predict that, for an arbitrary structure, if it contains the LHM layer (but not all), the reflected field passing through the LHM layer must be larger than that passing through the RHM case. Furthermore, the LHM-RHM PC will have the stronger influence on the inhibition or enhancement of the SpE than the ordinary PC.

It is known that the LHM-RHM PC has a near omnidirectional gap for the TE mode, while the ordinary PC hasn't [16]. In the following we will consider the quarter wavelength PC, the optical length of each layer being a quarter of one wavelength, because the quarter wavelength PC has a high reflectivity (or gap around centre frequency) in the normal direction. All layer Bs are the vacuum ($\varepsilon_B = 1.0$, $\mu_B = 1.0$) and $d_B = d_0 = \lambda_0/4$. For comparison, layer As can be LHM or RHM with the same absolute permittivity and permeability ($\varepsilon_A = \pm 2$, $\mu_A = \pm 0.5$, $|n_A|d_A = \lambda_0/4$). The total structure has the form $(0|A|(|B|A|)^4 0(|A|B|)^4|A|0)$. The reflectivity as function of frequency and incident angle are plotted in Figure 6.

In Figure 6, the white region implies nearly complete reflection. The lighter the color, the higher the reflectivity. Comparing with Figures 6a and 6b, we find that the LHM-RHM PC has a much wider gap than the ordinary PC not only in frequency but also in incident angle. Near $2\omega_0$, there is a resonant tunneling line in both cases. The difference between Figures 6a and 6b can be explained by the energy band theory used in reference [6], and also can

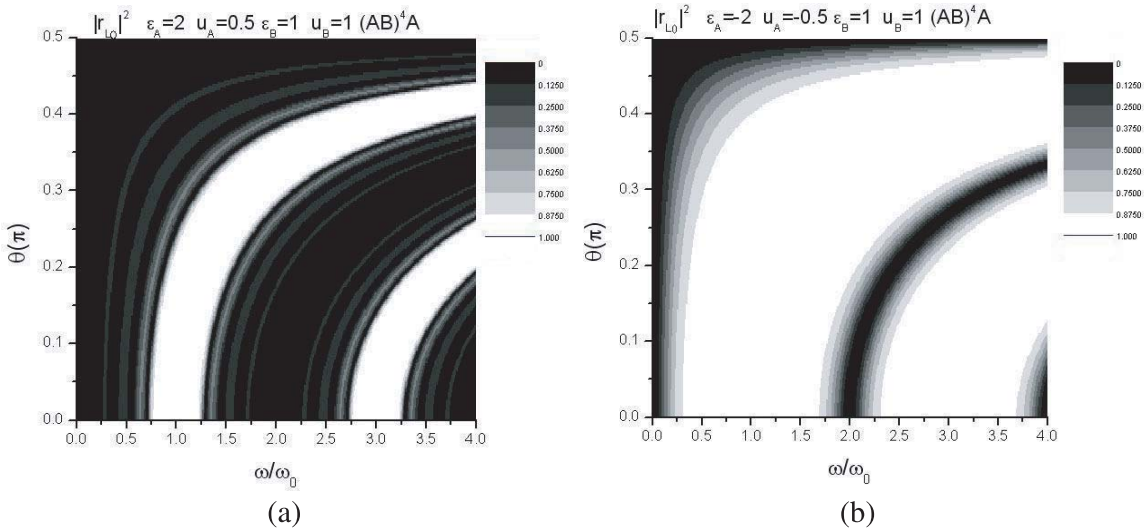

Fig. 6. The reflective index for TE waves versus frequency and incident angle for (a) RHM PC and (b) for LHM-RHM PC (TE and TM have no difference here).

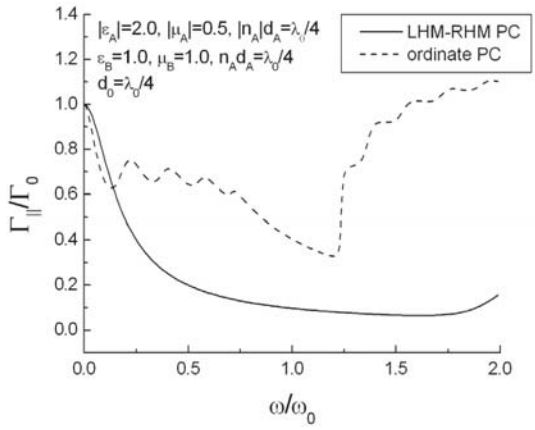

Fig. 7. The SpE rate as a function of ω when the atom lies between two symmetrical PCs ($(AB)^4A$).

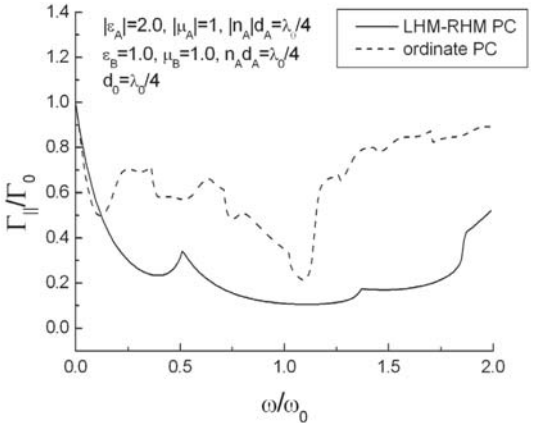

Fig. 8. The SpE rate as a function of ω when the atom lies between two symmetrical PCs ($(AB)^4A$).

be understood by the propagation analysis in the previous section. All the effects originate from the phase compensation effect of the LHM. It should be pointed out that, in Figure 6b, there is no omni-directional gap because the absolute refractive indexes are the same for each layer. The SpE rates of the atom with $\mathbf{p} = p(1, 0, 0)$ as function of frequency are drawn in Figure 7.

In Figure 7, the solid line and the dashed line are the SpE rates for the LHM-RHM PC and the ordinary PC, respectively. The SpE in the LHM-RHM PC is inhibited much more profoundly than in the ordinary PC in the frequency region near the gap. This is easy to understand by comparing Figure 6a with Figure 6b. High reflection means strong localization and fewer channels to propagate out. The LHM-RHM PC has a much wider gap than the ordinary PC both in frequency and in incident angle, which leads to a lower density of states within it.

A similar result is also obtained in other quarter wavelength PC ($|n_A|\, d_A = n_B d_B = d_0 = \lambda_0/4$) with the absolute value of the index not equal to 1. Consider the LHM-RHM PC and the ordinate PC with $\varepsilon_A = \pm 2$, $\mu_A = \pm 1$ for the layer A and the vacuum for the layer B ($\varepsilon_B = 1.0$, $\mu_B = 1.0$).

The SpE rate in the LHM-RHM PC is inhibited much stronger than in the ordinate PC at the frequency region near the gap, which is similar to Figure 7.

It should be noted that there is an apparent difference between the atomic decay in the F-P cavity and in the 1DPC. Though the 1DPC is a natural extension of the F-P cavity (by replacing the wall of the cavity by the 1DPC), the atomic decay is much more complicated in the 1DPC than in the F-P cavity due to the multiple reflection in each layer and the dependence of the reflectivity in the 1DPC on incident angles (the reflectivity at the wall of a cavity is taken to be a constant), which leads to less inhibition in the PC than in the F-P cavity, see dashed line in Figure 7 and 8. From Figure 6b, we can find that the reflectivity for the LHM-RHM PC is insensitive to the

angle θ at the frequency region near the gap, similar to the wall of the cavity, and the atomic steady decay rate is always inhibited more strongly in the LHM-RHM PC (see Figs. 7 and 8), which is similar to that in the cavity [14].

5 Conclusion

The spontaneous emission of the two-level atom located in a multi-layer structure containing LHM has been studied, and the results are compared with that in ordinary structure. In a three-layer structure, we find that the SpE rate oscillates with d_A for both the RHM layer A and the LHM layer A. The change of the SpE rate for the LHM case is much larger than that for RHM when d_A is small. Such a difference can be explained from the viewpoint of the reflected field which feed back to the atom. The reflected field passing through the LHM layer is stronger than that passing through the RHM layer. Due to the superposition (interference) of the reflected fields from all paths and the emitted field, the structure containing the LHM has a stronger effect on the atomic decay than the ordinary structure. Such a conclusion can be extended to the case of the quarter wavelength PCs. Compared with the case in the ordinary PC, the LHM-RHM PCs have a higher reflectivity which results in a strong suppression of the SpE under the appropriate conditions.

From our analysis, we find a new way to enhance or inhibit the atomic spontaneous decay without changing the dimension of the structure and it can be easily expanded to multi-atom interference.

It is necessary to point out the reason why we have not considered dispersion and dissipation. Firstly, the dispersion information will be lost with the Markov approximation and dispersion has no influence on the steady atomic decay. Secondly, the main difference between the LHM and the RHM is the opposite phase shift within them. However, the dissipation only provides a decay channel called non-radiated decay to the atom [13,17,18], and the non-radiated decay has no contribution to distinguish the different influences between the LHM and RHM. Introducing dissipation in the model just weaken the influence between the LHM and the RHM on the atomic decay, because only the propagating radiated field can distinguish the LHM from the RHM. When considering the non-Markov process, the dispersion of the LHM has to be taken into account, which will be done in further research.

This work was supported in part by the National Natural Science Fundation of China (No. 10674103), RGC from HK Government, FRC from HKBU, the Shanghai Phosphor Tracing Plan (No. 04QMH1407) and the foundation of Shanghai Science Committee.

Appendix: The evolution of $C_a(t)$ in the three-layer structure for a special case

For the symmetric structure ($r^{\lambda}_{L0} = r^{\lambda}_{R0} = r^{\lambda}_0$) and $\mathbf{p} = p(0,0,1)$, after inserting equations (9, 10) into equation (15), we get

$$\begin{aligned}\dot{C}_a(t) \approx & -\frac{3}{8\pi}\Gamma_0 \int_0^{\pi/2} d\theta \sin\theta \int_0^t dt' C_a(t') \\ & \times \int_{-\infty}^{\infty} d\nu_K e^{i(\omega_0-\nu_K)(t-t')} \left|t_0^{TE}\right|^2 \left|\frac{1+r_0^{TE}e^{iKd_0\cos\theta}}{D_0^{TE}}\right|^2 \\ & -\frac{3}{8\pi}\Gamma_0 \int_0^{\pi/2} d\theta \sin\theta\cos^2\theta \int_0^t dt' C_a(t') \\ & \times \int_{-\infty}^{\infty} d\nu_K e^{i(\omega_0-\nu_K)(t-t')} \left|t_0^{TM}\right|^2 \left|\frac{1+r_0^{TM}e^{iKd_0\cos\theta}}{D_0^{TM}}\right|^2, \end{aligned} \tag{A.1}$$

where $\Gamma_0 = p^2k^3/(3\varepsilon_0\pi\hbar)$ is the vacuum decay rate of the atom. In the above integration, K^2 is replaced by k_0^2 as it is not the exponential function. From equation (7), the last factor in the above equation can be rewritten as

$$\begin{aligned}|t_0^{\lambda}|^2 \left|\frac{1+r_0^{\lambda}e^{iKd_0\cos\theta}}{D_0^{\lambda}}\right|^2 = & 1+\sum_{n=1}^{\infty}(r_0^{\lambda}e^{iKd_0\cos\theta})^n \\ & +(r_0^{\lambda *}e^{-iKd_0\cos\theta})^n. \end{aligned} \tag{A.2}$$

In the derivation of (A.2), $\left|t_0^{\lambda}\right|^2 = 1-\left|r_0^{\lambda}\right|^2$ has been used due to lossless of all the layers. Inserting (A.2) into (A.1), we get

$$\begin{aligned}\dot{C}_a(t) = & \\ & -\frac{3}{8\pi}\Gamma_0 \int_0^{\pi/2} d\theta \sin\theta \int_0^t dt' C_a(t') \int_0^{\infty} d\nu_K e^{i(\omega_0-\nu_K)(t-t')} \\ & \times \left[1+\sum_{m=1}^{\infty}(r_0^{TE}e^{iKd_0\cos\theta})^m + (r_0^{TE*}e^{-iKd_0\cos\theta})^m\right] \\ & \qquad\qquad \mathbf{I}, \mathbf{II}, \mathbf{III} \\ & -\frac{3}{8\pi}\Gamma_0 \int_0^{\pi/2} d\theta \sin\theta\cos^2\theta \int_0^t dt' C_a(t') \int_0^{\infty} d\nu_K e^{i(\omega_0-\nu_K)(t-t')} \\ & \times \left[1+\sum_{m=1}^{\infty}(r_0^{TM}e^{iKd_0\cos\theta})^m + (r_0^{TM*}e^{-iKd_0\cos\theta})^m\right] \\ & \qquad\qquad \mathbf{IV}, \mathbf{V}, \mathbf{VI}. \end{aligned} \tag{A.3}$$

Next we will calculate the six integrations marked by **I**, **II**, **III**, **IV**, **V** and **VI** for $t \gg 1/\omega_0$. The following well-known results (valid for $t \gg 1/\omega_0$) are useful to perform

the next calculations

$$\int_0^t dt' C_a(t') \int_0^\infty d\nu_K e^{i(\omega_0-\nu_K)(t-t')} = \pi C_a(t) \tag{A.4a}$$

$$\int_0^t dt' C_a(t') \int_0^\infty d\nu_K e^{i(\omega_0-\nu_K)(t-t')} e^{imKd_0} = 2\pi e^{im\omega_0 d_0/c} C_a(t-md_0/c)\Theta(t-md_0/c) \tag{A.4b}$$

$$\int_0^t dt' C_a(t') \int_0^\infty d\nu_K e^{i(\omega_0-\nu_K)(t-t')} e^{-imKd_0} = 0. \tag{A.4c}$$

The most simplified example is the cavity formed by two single layers which its refractive index is 1 or -1 which we call it as special case. For example, $\varepsilon_A = 0.5$, $\mu_A = 2$ then $n_A = 1$, or $\varepsilon_A = -0.5$, $\mu_A = -2$ then $n_A = -1$. The advantage of such a case is that the reflectivity between each interface is independent of the incidence angle.

The total reflectivity of the layer can be expanded as

$$r_0^\lambda = r_{out}^\lambda + t_{in}^\lambda t_{out}^\lambda r_{in}^\lambda e^{2in_A Kd_A\cos\theta} \sum_{m=0}^\infty (r_{in}^{\lambda^2} e^{2in_A Kd_A\cos\theta})^m \quad \lambda = \text{TE or TM}. \tag{A.5}$$

According to Fresnel's law, note that $\cos\theta_A = \cos\theta_0$

$$\begin{aligned} r_{in}^{TE} &= \frac{n_A-\mu_A}{n_A+\mu_A}, & r_{in}^{TM} &= r_{in}^{TE}, \\ r_{out}^{TE} &= -r_{in}^{TE}, & r_{out}^{TM} &= -r_{in}^{TE}, \end{aligned} \tag{A.6}$$

where r_{in}^λ is the reflectivity incident from layer A to vacuum. r_{out}^λ is the reflectivity incident from vacuum to layer A

$$\begin{aligned} t_{in}^{TE} &= \frac{2\mu_A}{\mu_A+n_A}, & t_{in}^{TM} &= t_{in}^{TE}, \\ t_{out}^{TE} &= \frac{2n_A}{\mu_A+n_A}, & t_{out}^{TM} &= t_{out}^{TE}, \end{aligned} \tag{A.7}$$

where t_{out}^λ is the transmission incident from layer A to vacuum. t_{in}^λ is the transmission incident from vacuum to layer A.

We set

$$r_0 = r_{in}^{TE}, \quad t_0^2 = t_{in}^{TE} t_{out}^{TE} < 1 \tag{A.8}$$

and with the relationship between the different kinds of reflectivity and transmission in (A.6) and (A.7), we get

$$r_0^{TE} = -r_0 + t_0^2 r_0 e^{2in_A Kd_A\cos\theta} \sum_{m=0}^\infty (r_0^2 e^{2in_A Kd_A\cos\theta})^m \tag{A.9}$$

$$r_0^{TM} = r_0^{TE}. \tag{A.10}$$

Inserting (A.9) and (A.10) into (A.3), we can perform the six integrations in (A.3)

$$\begin{aligned} \mathbf{I}+\mathbf{IV} &= -\frac{1}{2\pi}\Gamma_0 \int_0^t dt' C_a(t') \int_0^\infty d\nu_K e^{i(\omega_0-\nu_K)(t-t')} \\ &= -\frac{\Gamma_0}{2} C_a(t) \end{aligned} \tag{A.11}$$

$$\begin{aligned} \mathbf{II} = -\frac{3}{8\pi}\Gamma_0 &\int_0^t dt' C_a(t') \int_0^\infty d\nu_K e^{i(\omega_0-\nu_K)(t-t')} \\ &\times \sum_{m=1}^\infty \int_0^{\pi/2} d\theta \sin\theta \left(r_0^{TE} e^{iKd_0\cos\theta}\right)^m. \end{aligned} \tag{A.12}$$

For equation (A.9), we only retain the terms up to r_0^2. So that

$$\begin{aligned} r_0^{TE} e^{iKd_0\cos\theta} &\approx -r_0 e^{iKd_0\cos\theta} \\ &\quad + t_0^2 r_0 e^{2in_A Kd_A\cos\theta} e^{iKd_0\cos\theta} \\ (r_0^{TE})^2 e^{2iKd_0\cos\theta} &\approx r_0^2 e^{2iKd_0\cos\theta} \\ &\quad - 2t_0^2 r_0^2 e^{2in_A Kd_A\cos\theta} e^{2iKd_0\cos\theta} \\ &\quad + t_0^4 r_0^2 e^{4in_A Kd_A\cos\theta} e^{2iKd_0\cos\theta}. \end{aligned}$$

Consequently, we have

$$\begin{aligned} \sum_{m=1}^\infty \left(r_0^{TE} e^{iKd_0\cos\theta}\right)^m &\approx \sum_{m=1}^2 \left(-r_0 e^{iKd_0\cos\theta}\right)^m \\ &\quad + \sum_{m=1}^2 \left(t_0^2 r_0 e^{2in_A Kd_A\cos\theta} e^{iKd_0\cos\theta}\right)^m \\ &\quad - 2t_0^2 r_0^2 e^{2in_A Kd_A\cos\theta} e^{i2Kd_0\cos\theta} \end{aligned} \tag{A.13}$$

$$\begin{aligned} \mathbf{III} = -\frac{3}{8\pi}\Gamma_0 &\int_0^t dt' C_a(t') \int_0^\infty d\nu_K e^{i(\omega_0-\nu_K)(t-t')} \\ &\times \sum_{m=1}^\infty \int_0^{\pi/2} d\theta \sin\theta \left(r_0^{TE} e^{-imKd_0\cos\theta}\right)^{*m}. \end{aligned} \tag{A.14}$$

Similarly the sum can be written as

$$\begin{aligned} \sum_{m=1}^\infty \left(r_0^{TE} e^{iKd_0\cos\theta}\right)^{*m} &\approx \sum_{m=1}^2 \left(-r_0 e^{-iKd_0\cos\theta}\right)^m \\ &\quad + \sum_{m=1}^2 \left(t_0^2 r_0 e^{-2in_A Kd_A\cos\theta} e^{-iKd_0\cos\theta}\right)^m \\ &\quad - 2t_0^2 r_0^2 e^{-2in_A Kd_A\cos\theta} e^{i2Kd_0\cos\theta}. \end{aligned} \tag{A.15}$$

$$\dot{C}_a(t) \approx -\frac{\Gamma_0}{2}C_a(t) - \frac{3}{4}\Gamma_0 Re\sum_{m=1}^{2}\left((-r_0)^m e^{imk_0d_0}\left[\frac{2}{imk_0d_0}+\frac{2}{(mk_0d_0)^2}-\frac{2}{i\,(mk_0d_0)^3}\right]\right)C_a(t) - \frac{3}{4}\Gamma_0 Re\sum_{m=1}^{2}\left((t_0^2r_0)^m e^{im(2n_Ak_0d_A+k_0d_0)}\left[\frac{2}{im(2n_Ak_0d_A+k_0d_0)}+\frac{2}{m^2(2n_Ak_0d_A+k_0d_0)^2}-\frac{2}{im^3(2n_Ak_0d_A+k_0d_0)^3}\right]\right)C_a(t) - \frac{3}{4}\Gamma_0 Re\sum_{m=1}^{2}(-2t_0^2r_0^2)^m e^{im(2n_Ak_0d_A+2k_0d_0)}\left[\frac{2}{i(2n_Ak_0d_A+2k_0d_0)}+\frac{2}{(2n_Ak_0d_A+2k_0d_0)^2}-\frac{2}{i(2n_Ak_0d_A+2k_0d_0)^3}\right]C_a(t) + \ldots \quad \text{(A.18)}$$

$$\Gamma \approx \Gamma_0 + \frac{3}{2}\Gamma_0 Re\sum_{m=1}^{2}\left((-r_0)^m e^{imk_0d_0}\left[\frac{2}{imk_0d_0}+\frac{2}{(mk_0d_0)^2}-\frac{2}{i\,(mk_0d_0)^3}\right]\right) + \frac{3}{2}\Gamma_0 Re\sum_{m=1}^{2}\left((t_0^2r_0)^m e^{im(2n_Ak_0d_A+k_0d_0)}\left[\frac{2}{im(2n_Ak_0d_A+k_0d_0)}+\frac{2}{m^2(2n_Ak_0d_A+k_0d_0)^2}-\frac{2}{im^3(2n_Ak_0d_A+k_0d_0)^3}\right]\right) + \frac{3}{2}\Gamma_0 Re\sum_{m=1}^{2}(-2t_0^2r_0^2)^m e^{im(2n_Ak_0d_A+2k_0d_0)}\left[\frac{2}{i(2n_Ak_0d_A+2k_0d_0)}+\frac{2}{(2n_Ak_0d_A+2k_0d_0)^2}-\frac{2}{i(2n_Ak_0d_A+2k_0d_0)^3}\right] + \ldots \quad \text{(A.19)}$$

The result of **IV** and **V** can be obtained in a similar way. With the help of (A.4) and the following two formulas,

$$\int_0^{\pi/2} d\theta \sin\theta e^{iF\cos\theta} = \int_0^1 dx e^{iFx} = \frac{e^{iF_0}-1}{iF} \quad \text{(A.16)}$$

$$\int_0^{\pi/2} d\theta \sin\theta\cos^2\theta e^{imKd_0\cos\theta} = e^{imKd_0}\left[\frac{1}{imKd_0} + 2\frac{1}{(mKd_0)^2} - 2\frac{1}{i\,(mKd_0)^3}\right] + \frac{2}{i\,(mKd_0)^3} \quad \text{(A.17)}$$

and note that $C_a(t-md_n/c) \approx C_a(t)$at $t \gg 1/\omega_0$, we get the final equation for (A.3) without the Lamb shift

see equation (A.18) above

and the steady decay rate can be written as

see equation (A.19) above.

References

1. V.G. Veselago, Sov. Phys. Usp. **10**, 509 (1968)
2. D.R. Smith, W.J. Padilla, D.C. Vier, S.C. Nemat-Nasser, S. chultz, Phys. Rev. Lett. **84**, 4184 (2000)
3. G.V. Eleftheriades, A.K. Iyer, P.C. Kremer, IEEE Trans. Microw. Theory, Techn. **50**, 2702 (2002); C.G. Parazzoli, R.B. Greegor, K. Li, B.E.C. Koltenbah, M. Tanielian, Phys. Rev. Lett. **90**, 10740(2003)
4. V. Yannopapas, A. Moroz, J. Phys.: Condens. Matter **17**, 3717 (2005); M.S. Wheeler, J.S. Aitchison, M. Mojahedi, Phys. Rev. B **73**, 045105 (2005)
5. J.B. Pendry, Phys. Rev. Lett. **85**, 3966 (2000)
6. J. Li, L. Zhou, C.T. Chan, P. Sheng, Phys. Rev. Lett. **90**, 083901 (2003)
7. E.M. Purcell, Phys. Rev. **69**, 681 (1946)
8. S.-Y. Zhu, Y. Yang, H. Chen, H. Zheng, M.S. Zubairy, Phys. Rev. Lett. **84**, 2136 (2000)
9. Y. Yang, S.-Y. Zhu, Phys. Rev. A **62**, 013805 (2000)
10. Y. Yang, M. Fleischhauer, S.-Y. Zhu, Phys. Rev. A **68**, 043805 (2003)
11. H.T. Dung, S. Y. Buhmann, L. Knöll, D.-G. Welsch, Phys. Rev. A **68**, 043816 (2003)
12. S. Scheel, L. Knöll, D.-G. Welsch, Phys. Rev. A **60**, 1590 (1999)
13. H.T. Dung, L. Knöll, D.-G Welsch, Phys. Rev. A **62**, 053804 (2000)
14. F. De Martini, M. Marrocco, P. Mataloni, L. Crescentini, R. Loudon, Phys. Rev. A **43**, 2480 (1991)
15. M.O. Scully, M. Suhail Zubairy, *Quantum Optics* (Cambridge University Press, 1997)
16. H. Jiang, H. Chen, H. Li, Y.W. Zhang, Appl. Phys. Lett. **83,** 05386 (2003)
17. M.S. Tomas, Z. Lenac, Phys. Rev. A **56**, 4197 (1997)
18. S. Scheel, L. Knöll, D.-G. Welsch, Phys. Rev. A **60**, 4094 (1999)